Model based Online Fault Diagnosis of Automotive Engines using Joint State and Parameter Estimation

Nadeer E P[1], Amit Patra[2], and Siddhartha Mukhopadhyay[3]

[1,2,3] *Indian Institute of Technology, Kharagpur, West Bengal, 721302, India*

epnadeer@iitkgp.ac.in
amit@ee.iitkgp.ernet.in
smukh@ee.iitkgp.ernet.in

ABSTRACT

In this work, an Extended Kalman Filter (EKF) based tunable diagnoser, which uses a minimal hybrid nonlinear state space model of a spark ignition (SI) four stroke engine, is used for the detection and isolation of a variety of engine system faults including intake manifold leak, injector fault and exhaust manifold leak. The state estimates and innovation sequences from the EKF based estimator are shown to be adequate for the detection and isolation of the faults under consideration. Once a fault is detected and isolated, the diagnoser could be tuned online to perform fault identification by redefining a model/fault parameter as an additional state to be estimated, and then performing a joint state and parameter estimation. The engine model and diagnoser are implemented in Simulink™ and are validated against an AMESim™ model of the engine. For the nominal engine model, the performance of the EKF estimator is compared with two other computationally more expensive nonlinear estimators, namely the Unscented Kalman Filter (UKF) and Rao-Blackwell Particle Filter (RBPF).

1. INTRODUCTION

Traditionally, automotive engine modelling has been carried out using Mean value engine models (MVEMs). MVEMs are formulated based on the assumption that all processes and effects are spread out over the entire engine cycle, and do not take into account the reciprocating nature of the engine (Guzzella & Onder, 2010). An alternative to MVEM, which takes into account the within-cycle reciprocating nature of the engine cylinders, is the Within Cycle Crank-angle-based Model (WCCM) (Sengupta S. , Mukhopadhyay, Deb, Pattada, & De, 2012). WCCMs are instantaneous physics-based models and have the advantage of being able to detect, isolate and identify small faults within shorter time duration as compared with MVEMs. This, however, comes at a greater computational effort.

WCCM based fault diagnosis of engines has been carried out using a bank of Extended Kalman Filters (EKF) in (Sengupta, Mukhopadhyay, & Deb, 2011). However, presence of multiple estimators and calculation of Jacobian matrix by simulation makes the use of such bank of estimators prohibitive for online implementation in a real time fault diagnosis system for engines. In this work, these shortcomings are overcome by three modifications. Firstly, a minimal hybrid state space model is derived by reformulating the mass and energy balance equations. Secondly, the EKF uses analytically derived expressions for the Jacobian matrix instead of employing simulation to find it. Finally, instead of a bank of estimators, a single tunable estimator is employed for fault diagnosis. The estimator identifies a fault parameter only when a fault is detected and/or isolated using the residuals and state estimates from a nominal EKF.

Figure 1 shows the proposed fault diagnosis framework. The control inputs from the Engine Control Unit (ECU) and measurements from the engine are inputs to the estimator. Fault-detection and isolation (FDI) logic monitors the state estimates and residuals (innovation sequence) from the estimator. Once a fault is detected and isolated, the FDI sends commands to the estimator for identification of the concerned parameter(s). A joint state and parameter estimation is then performed to identify the fault magnitude. The estimation accuracy depends on the input conditions also.

2. ENGINE MODELING, ESTIMATION AND FAULT DIAGNOSIS

In this section, the minimal hybrid state space modeling of the engine, nonlinear estimation of engine states, the fault detection and isolation methodology and the fault identification method using joint state and parameter estimation are described.

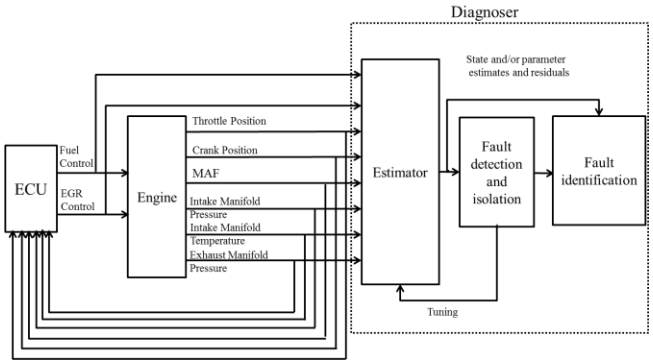

Figure 1. The proposed fault diagnosis framework

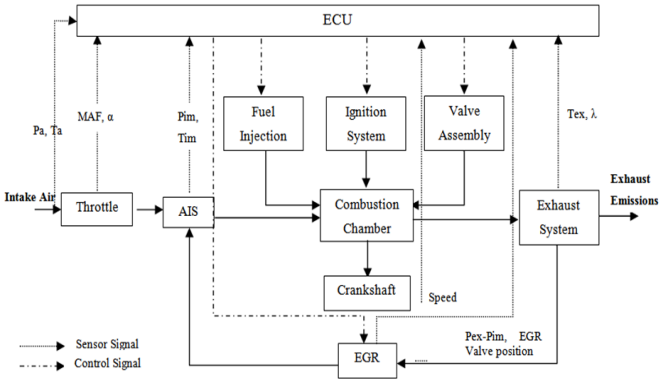

Figure 2. Block diagram of an SI engine

2.1. Minimal hybrid state space model of the engine

A naturally aspirated spark ignition (SI) gasoline engine has the basic subsystems and components shown in Figure 2, which include the intake manifold, combustion chamber (cylinder and piston), exhaust manifold, crank assembly, Exhaust gas recirculation (EGR), ECU, fuel injection and sensor and actuator assembly. A physical system such as an engine consists of two kinds of objects: reservoirs and flows. Reservoirs store thermal or kinetic energy, mass, information, etc., whereas flows have these storage entities flowing between reservoirs, typically driven by differences in reservoir levels (Guzzella & Onder, 2010). In the case of the engine, we consider the intake manifold (IM) or Air Intake System (AIS), cylinder and exhaust manifold (EM) as reservoirs. The throttle, exhaust gas recirculation (EGR) and muffler are considered as flow elements. The equations we use here are from standard models available in duly mentioned references, the novelty is only in the state space formulation. We start the development by considering the regular direction of mass and energy – from throttle to exhaust.

A full 4-stroke engine cycle corresponds to a crank shaft rotation of 0-720°, approximately 180° each for intake, compression, expansion and exhaust strokes. The WCCM equations essentially describe two things: the continuous time dynamics (or flows) of the variables or system states of interest – such as pressure, temperature and mass flow rates – and the jump conditions, or events, which cause transition between different modes of the hybrid system. These transitions between modes could be triggered either by control actions or by the instantaneous state variable values themselves (e.g., sub-sonic or sonic, positive flow or negative flow).

We assume that all the gases in the engine obey the ideal gas law, i.e.,

$$PV = mRT \text{ or } P = mRT/V \tag{1}$$

(Please refer to nomenclature section for symbols and notations).

The differential equations describing the reservoir can be written in terms of the mass m, the internal energy U, the enthalpy H and the heat energy Q, as:

$$\begin{aligned} \dot{m} &= \dot{m}_{in} - \dot{m}_{out} \\ \dot{U} &= \dot{H}_{\text{in}} - \dot{H}_{\text{out}} + \dot{Q}_{in} - \dot{Q}_{out} \end{aligned} \tag{2}$$

The subscripts *in* and *out* respectively denote variables entering and leaving the reservoir. The flow equation for valves can be written as (Guzzella & Onder, 2010):

$$\dot{m} = C_d A \frac{P_{\text{in}}}{\sqrt{R_{\text{in}} T_{\text{in}}}} \psi\left(\frac{P_{\text{in}}}{P_{\text{out}}}\right) \tag{3}$$

where, and

$$\psi\left(\frac{P_{\text{in}}}{P_{\text{out}}}\right) = \begin{cases} \sqrt{\gamma_{\text{in}}\left[\frac{2}{\gamma_{\text{in}}+1}\right]^{\frac{\gamma_{\text{in}}+1}{\gamma_{\text{in}}-1}}}, & P_{\text{out}} < P_{\text{cr}} \\ \left(\frac{P_{\text{out}}}{P_{\text{in}}}\right)^{\frac{1}{\gamma_{\text{in}}}} \sqrt{\frac{2\gamma_{\text{in}}}{\gamma_{\text{in}}-1}\left[1-\left(\frac{P_{\text{out}}}{P_{\text{in}}}\right)^{\frac{\gamma_{\text{in}}-1}{\gamma_{\text{in}}}}\right]}, & P_{\text{out}} \geq P_{\text{cr}} \end{cases}$$

$$P_{cr} = 2/(\gamma_{in}+1)^{\frac{\gamma_{in}}{\gamma_{in}-1}} P_{in} \ .$$

P_{in} and P_{out} will be interchanged and γ_{in} values will be replaced by γ_{out} for reverse flow (negative).

The model inputs are: Throttle position, Fuel control signal, EGR control signal, speed and crank angle.

At each storage element, we approximate the specific gas constant R (for air, burnt gases and fuel) and specific heats C_p and C_v in terms of mass fractions as:

$$R = \frac{\sum m_i R_i}{m},\ C_p = \frac{\sum m_i C_{pi}}{m},\ C_v = \frac{\sum m_i C_{vi}}{m},\ \gamma = C_p / C_v \tag{4}$$

Where, $i=a,b,f$ (for air, burnt gases and fuel), and $m = m_a + m_b + m_f$.

The time derivatives of internal energy and enthalpy can be expressed in terms of masses, specific heats and temperature as:

$$\dot{U} = mC_v\dot{T} + m\dot{C}_vT + \dot{m}C_vT$$
$$\dot{H} = mC_p\dot{T} + m\dot{C}_pT + \dot{m}C_pT \quad (5)$$

We choose a minimal state vector as:

$$x = \left[m_{im,i}, T_{im}, m_{cyl,i}, T_{cyl}, m_{em,i}, T_{em} \right]^T \quad (6)$$

where, *i = a,b,f (air, burnt gases, fuel)*. Throughout this paper, subscripts *im*, *cyl* and *em* stand for intake manifold, cylinder and exhaust manifold respectively. m_{cyl} and T_{cyl} are vectors with elements denoting the mass and temperature for individual cylinders. It will be shown that by this choice of state, it is possible to express the nonlinear engine dynamical equations in the form $\boldsymbol{x} = \boldsymbol{f}(\boldsymbol{x}, \boldsymbol{u}, \boldsymbol{t})$, where u is the input vector.

2.1.1. Intake and exhaust manifold states

The mass balance at IM is:

$$\dot{m}_{\text{im}} = \dot{m}_{\text{th}} + \dot{m}_{\text{egr}} - \dot{m}_{\text{i2c}} \quad (7)$$

Where m_{th} and m_{egr} stand for the mass flow rates at throttle and EGR respectively, and m_{i2c} is the flow rate of gas entering the cylinder from IM. These can be obtained at every time instant by using the flow equation in Eq. (3). Replacing the pressures P_{in} and P_{out} in Eq. (3) by Eq. (1), and the ratio of specific heats γ_{in} from Eq. (4), it can be seen that all the terms in Eq. (7) are expressed purely in terms of the states in Eq. (6). The individual mass flow rates m_i for air, burnt gases and fuel can be obtained from the above relation by multiplying each of these flow rates by the individual fractions from the previous time instant. Considering m_i as states, from Eqs. (1) and (4) it follows that only one of *P* and *T* needs to be considered as a state, since the other could then be obtained by an algebraic relation.

The dynamics for temperature *T* at the IM can be obtained from enthalpy balance in Eq. (2), assumptions on C_p and C_v in Eq. (4) and the thermodynamic expressions for enthalpy and internal energy as:

$$\dot{T}_{im} = \frac{1}{m_{im}C_{v_{im}}} \begin{pmatrix} \dot{m}_{th}(\sigma_{\dot{m}_{th}} C_{p_a} T_a + (1-\sigma_{\dot{m}_{th}}) C_{p_{im}} T_{im}) \\ +\dot{m}_{egr}(\sigma_{\dot{m}_{egr}} C_{p_{em}} T_{em} + (1-\sigma_{\dot{m}_{egr}}) C_{p_{im}} T_{im}) \\ -\sum_{i=1}^{N} \left(\dot{m}_{i2c,i} \left(\sigma_{\dot{m}_{i2c,i}} C_{p_{im}} T_{im} + (1-\sigma_{\dot{m}_{i2c,i}}) C_{p_{cyl,i}} T_{cyl,i} \right) \right) \\ -h_{c,im} A_{c,im} \left(T_{im} - T_{cool,im} \right) - \dot{m}_{im} C_{v_{im}} T_{im} \end{pmatrix} \quad (8)$$

where $\sigma_{\dot{m}} = \left(\frac{1+\text{sgn}[\dot{m}]}{2} \right)$, sgn(.) denoting the signum function and *N* is the number of cylinders . The heat energy lost due to convection is also included in the above equation.

Mass and energy balance at the exhaust manifold gives similar expressions:

$$\dot{m}_{\text{em}} = \dot{m}_{c2e} - \dot{m}_{\text{egr}} - \dot{m}_{\text{muf}} \quad (9)$$

where m_{c2e} is the cylinder-to-exhaust flow rate and m_{muf} is the muffler flow rate.

$$\dot{T}_{em} = \frac{1}{m_{em}C_{v_{em}}} \begin{pmatrix} \sum_{i=1}^{N} \left(\dot{m}_{c2e,i} \left(\sigma_{\dot{m}_{c2e,i}} C_{p_{cyl,i}} T_{cyl,i} + (1-\sigma_{\dot{m}_{c2e,i}}) C_{p_{em}} T_{em} \right) \right) \\ -\dot{m}_{muf}(\sigma_{\dot{m}_{muf}} C_{p_{em}} T_{em} + (1-\sigma_{\dot{m}_{muf}}) C_{p_a} T_a) \\ -\dot{m}_{egr}(\sigma_{\dot{m}_{egr}} C_{p_{em}} T_{em} + (1-\sigma_{\dot{m}_{egr}}) C_{p_{im}} T_{im}) \\ -h_{c,em} A_{c,em} \left(T_{em} - T_{cool,em} \right) - \dot{m}_{em} C_{v_{em}} T_{em} \end{pmatrix} \quad (10)$$

2.1.2. Cylinder states

The mass balance equation for individual cylinders could be written as:

$$\dot{m}_{\text{cyl}} = \dot{m}_{\text{i2c}} - \dot{m}_{\text{c2e}} + \dot{m}_f \quad (11)$$

Where m_f is the fuel input flow rate. During combustion, the total mass flow rate is zero, but the air and fuel get converted to burnt gases, changing individual component rates. These rates can be calculated for the i^{th} cylinder as:

$$\begin{aligned} \dot{m}^{(i)}_{cyl,a} &= \dot{m}^{(i)}_{i2c} \left(\sigma_{\dot{m}^{(i)}_{i2c}} \frac{m_{im,a}}{m_{im}} + (1-\sigma_{\dot{m}^{(i)}_{i2c}}) \frac{m^{(i)}_{\text{cyl},a}}{m^{(i)}_{cyl}} \right) \\ &- \dot{m}^{(i)}_{c2e} \left(\sigma_{\dot{m}^{(i)}_{c2e}} \frac{m^{(i)}_{\text{cyl},a}}{m^{(i)}_{cyl}} + (1-\sigma_{\dot{m}^{(i)}_{c2e}}) \frac{m_{em,a}}{m_{em}} \right) - \frac{m^{(i)}_{fb} \lambda_{af} \omega}{\Delta\theta} \\ \dot{m}^{(i)}_{cyl,f} &= \dot{m}^{(i)}_{i2c} \left(\sigma_{\dot{m}^{(i)}_{i2c}} \frac{m_{im,f}}{m_{im}} + (1-\sigma_{\dot{m}^{(i)}_{i2c}}) \frac{m^{(i)}_{\text{cyl},f}}{m^{(i)}_{cyl}} \right) \\ &- \dot{m}^{(i)}_{c2e} \left(\sigma_{\dot{m}^{(i)}_{c2e}} \frac{m^{(i)}_{\text{cyl,f}}}{m^{(i)}_{cyl}} + (1-\sigma_{\dot{m}^{(i)}_{c2e}}) \frac{m_{em,\text{f}}}{m_{em}} \right) - \frac{m^{(i)}_{fb} \omega}{\Delta\theta} + \dot{m}^{(i)}_f \\ \dot{m}^{(i)}_{cyl,b} &= \dot{m}^{(i)}_{cyl} - \dot{m}^{(i)}_{cyl,a} - \dot{m}^{(i)}_{cyl,f} \end{aligned} \quad (12)$$

Where $m^{(i)}_{fb}$ is the mass of fuel accumulated in cylinder *i* before combustion, ω is the engine angular speed, λ_{af} is the stoichiometric air-fuel ratio and $\Delta\theta$ is the combustion duration angle.

In addition to the terms in enthalpy balance for IM and EM, the enthalpy balance for the cylinder should include the heat energy added during combustion – approximated by the Wiebe function (Heywood, 1998) – and lost due to radiation (Annand, 1963), given by:

$$\begin{aligned} \dot{Q}^{(i)}_{comb} &= \eta^{(i)}_c m^{(i)}_f Q_{LHV} \omega \frac{dx^{(i)}_b}{d\theta} \\ &= \frac{\eta^{(i)}_c m^{(i)}_f Q_{LHV} \omega n a}{\Delta\theta} \left(\frac{\theta - \theta_{soc}}{\Delta\theta} \right)^{n-1} \exp\left[-a \left(\frac{\theta - \theta_{soc}}{\Delta\theta} \right)^n \right] \end{aligned} \quad (13)$$

$$\dot{Q}^{(i)}_{heatloss} = h^{(i)}_c A^{(i)}_c (T^{(i)}_c - T^{(i)}_{cool}) + \varepsilon\sigma \left((T^{(i)}_c)^4 - (T^{(i)}_{cool})^4 \right)$$

Further, from the first law of thermodynamics, the mechanical work done should be subtracted from the heat energy added to get the change in internal energy. Thus for the i^{th} cylinder, the expression for cylinder temperature derivative is:

$$\dot{T}_c^{(i)} = \frac{1}{m_{cyl}^{(i)} C v_{cyl}^{(i)}} \begin{bmatrix} \dot{Q}_{comb}^{(i)} - \dot{Q}_{heatloss}^{(i)} + \dot{H}_{in}^{(i)} - \dot{H}_{out}^{(i)} \\ -T_c^{(i)} \times \left(\dot{m}_{cyl}^{(i)} C v_{cyl}^{(i)} + m_{cyl}^{(i)} \dot{C} v_{cyl}^{(i)} \right) - P_c^{(i)} \dot{V}_c^{(i)} \end{bmatrix} \quad (14)$$

The state space formulation requires that all the variables be expressed in terms of states and their first order derivatives. Eqs. (1) and (4) can be used to express P_c and C_{vcyl} as algebraic states. However, the derivative of C_{vcyl} should be expressed in terms of the states and their derivatives only. To this end, from the assumptions made in Eqs. (4) and (5), we write:

$$\dot{m}_{cyl} C v_{cyl} + m_{cyl} \dot{C} v_{cyl} = \sum_i \dot{m}_{cyl,i} C_{v,i}$$

Where, *i = a,b,f (air, burnt gases, fuel)*

A similar technique could be used for the derivatives of enthalpy terms H which in turn depend on the derivatives of C_{pcyl}. Further, if the cylinder dimensions are known, the derivative of the cylinder volume, V_c, in the above equation can be expressed as a function of angular speed. Hence, all of the terms in the right hand side of Eq. (14) can be expressed as a function of states only, and without their derivatives. Eqs. (7)-(14) constitute the first order non-linear differential equations necessary for forming the state space model.

2.2. Estimation of Nominal Engine States

The engine model equations described in the previous section are nonlinear and hybrid in nature. However, the model exhibits no state resets when transitioning from one discrete mode to other. The optimal state estimation problem of nonlinear systems is intractable for many practical problems. Hence extensions of linear system techniques for state estimation, like the Kalman filter (KF), are often used in practice. The most common techniques in use are the Extended Kalman Filter (EKF), the Unscented Kalman Filter (UKF) and their variants. For hybrid systems, the optimal estimation of discrete modes and continuous states would mean that the number of modes to be estimated grows exponentially with each time step. To reduce the complexity, in some techniques, N modes with largest probability are kept and the rest are discarded, and probabilities are renormalized to sum up to unity (Bar-Shalom, Li, & Kirubarajan, 2004). The generalized pseudo-Bayesian (GPB) approaches and interacting multiple model (IMM) estimation (Bar-Shalom, Li, & Kirubarajan, 2004) fall in this category. Particle filters (PF) (Doucet, De Freitas, Gordon, & others, 2001), (Arulampalam, Maskell, Gordon, & Clapp, 2002) are a class of numerical methods for the solution of the optimal estimation problem in non-linear non-Gaussian scenarios and come under the generic name Sequential Monte Carlo algorithms. In UKF, the weights for the sigma points are fixed, whereas in PF, the weights of particles are dependent on the posterior probabilities, and hence can be expected to perform better. The Rao-Blackwell particle filter (RBPF) is a special kind of particle filter that reduces the variance in estimates. Specifically, the estimation state space is partitioned so that one set is updated with sampling whereas the other set is updated analytically using KF, EKF or UKF. In the hybrid estimation problem, the RBPF has been applied with sampling for discrete states and exact computations of mean and variances using KF for continuous states (De Freitas, 2002). In our case, the particles do not have a one-to-one correspondence with discrete modes.

In this work, sensor measurements that are assumed to be available to the estimator are: throttle position (from which throttle area could be found out), IM pressure, IM temperature, EM pressure and EM temperature. The engine speed and crank angle are considered to be inputs. In the case of an actual engine, these signals have to be derived from the crank position sensor signal. The estimator is a continuous-discrete one, i.e., the engine dynamical equations are continuous, but measurements are assumed to be discrete. The integration of continuous dynamics has been carried out using RK4 method. Estimation of nominal engine states has been carried out using EKF, UKF and RBPF and results were compared. The EKF uses analytical expressions for the Jacobian matrix entries.

2.2.1. The EKF Algorithm (Sarkka, 2006)

Prediction: Integrate the following differential equations to get m_k^- and P_k^-:

$$\begin{aligned} \dot{x} &= f(x,u) \\ \dot{P}_t &= F P_t + P_t F' + Q_t \end{aligned} \quad (15)$$

Where F is the Jacobian of f *w.r.t* the state vector x, Q_t is the process noise covariance and P_t is the estimation error covariance. Variables x and P_t are assigned the values m_{k-1} and P_{k-1} from previous time step before solving the above equations.

Update:

$$\begin{aligned} v_k &= y_k - h(m_k^-) \\ S_k &= H_k P_k^- H_k' + R_k \\ K_k &= P_k^- H_k' S_k^{-1} \\ m_k &= m_k^- + K_k v_k \\ P_k &= P_k^- - K_k S_k K_k' \end{aligned} \quad (16)$$

Where *h(.)* denotes the measurement function and *H*, its Jacobian. R_k is the measurement noise covariance.

2.2.2. The RBPF Algorithm (Hutter, Dearden, & others, 2003)

1. For N particles $p^{(i)}, i = 1:N$, sample discrete modes $z_0^{(i)}$ from the prior $P(Z_0)$
2. For each particle $p^{(i)}$, set μ_0^i, Σ_0^i to the prior mean and variance in state $z_0^{(i)}$
3. For each time-step t do
   a) For each particle $p^{(i)} = \left(z_{t-1}^{(i)}, x_{t-1}^{(i)}\right)$ do
      i) Sample a new mode:
      $\hat{z}_t^{(i)} \sim P\left(Z_t / z_{t-1}^{(i)}\right)$
      ii) Perform EKF update using parameters from mode $\hat{z}_t^{(i)}$
      $(\hat{y}_{t/t-1}^{(i)}, \hat{S}_t^{(i)}, \hat{\mu}_t^{(i)}, \hat{\Sigma}_t^{(i)}) \leftarrow EKF(\mu_{t-1}^{(i)}, \Sigma_{t-1}^{(i)}, y_t)$
      iii) Compute the weight of particle $p^{(i)}$:
   b) Resample *N* new samples $p^{(i)}$ where:
   $P(p^{(i)} = \hat{p}^{(k)}) \propto w_t^{(k)}$

2.3. Fault Modelling

In this work, three faults are considered: intake manifold leak, fuel injector choking, and exhaust manifold leak. The IM leak could be modelled by an additional leak area in the throttle flow orifice equation. The injector fault could be modelled by changing the fuel injector signal to one of the cylinders. In our case the fuel injection duration was halved. The exhaust manifold leak can be modelled by an additional area in the muffler flow equation.

2.4. Online Fault Detection and Isolation

The fault detection algorithm assumes that only one fault occurs at a time. This is not unreasonable, because the algorithm tries to detect faults early using an instantaneous model, and hence it is very unlikely for multiple faults to occur at exactly the same sampling instant. To enhance the prospects of online implementation, only one estimator, namely the one for the nominal case, runs at a time. The fault detection and isolation algorithm monitors the measurement residuals and states from the estimator. An estimator which considers all the fault parameters as states to be estimated will have very poor observability because of the fewer measurements compared to the number of states.

Part of the fault detection logic runs with the nominal estimator and tries to predict the measurement residuals in presence of single faults, captured by corresponding parameters. For example, the intake manifold leak can be captured by an additional area in the throttle. By defining this area to be a parameter, it is possible to predict the fault residuals in presence of IM leak. A similar method could be adopted for EM leak with the muffler area. If w_i is the parameter associated with fault *i*, and Δw_i a small change in w_i, indicating a fault, then from Eq.(16) we can predict the residual for fault *i* as:

$$\Delta v_k^i = -\left(\frac{\partial h}{\partial m_k^-}\frac{\partial m_k^-}{\partial w_i} + \frac{\partial h}{\partial w_i}\right)\Delta w_i \tag{17}$$

Note that $\frac{\partial h}{\partial m_k^-} = H_k$, which is already available from the EKF routine. The term $\frac{\partial m_k^-}{\partial w_i}$ could be calculated recursively by a technique similar to dual estimation in (Haykin, 2001):

$$\begin{aligned}\frac{\partial m_{k+1}^-}{\partial w_i} &= \left(I + \frac{\partial f}{\partial m_k}\Delta T\right)\frac{\partial m_k}{\partial w_i} + \frac{\partial f}{\partial w_i}\Delta T \\ \frac{\partial m_k}{\partial w_i} &= \frac{\partial m_k^-}{\partial w_i} - K\left(\frac{\partial h}{\partial m_k^-}\frac{\partial m_k^-}{\partial w_i} + \frac{\partial h}{\partial w_i}\right)\end{aligned} \tag{18}$$

Where we have discretized the continuous dynamics by Euler approximation. *K* is the Kalman gain and ΔT is the sampling interval. Note that $\frac{\partial f}{\partial m_k} = F$, already available from EKF routine in Eq. (15).

If the sign-reversed residual from the estimator is Δv_k, and a fault of magnitude Δw_i is present, we expect Δv_k to be approximately equal to Δv^i_k. However, in actual case, neither the fault type nor its magnitude is known. An intuitive way to detect the fault is to normalize both Δv_k and Δv^i_k, calculate a moving average (with window length *M*) of their inner product, and choose the fault *i* for which the inner product is maximum:

$$\begin{aligned} g_k &= \sum_{k-M+1}^{k} \frac{(\Delta v_k)^T \Delta v_k^i}{\|\Delta v_k\|\|\Delta v_k^i\|} \\ fault\ index &= \arg\max_i g_k \end{aligned} \tag{19}$$

The above condition is applied only when the products are more than a set threshold value between 0 and 1. Otherwise, a fault free condition is inferred. To save memory, the moving average filter could be replaced by an Infinite Impulse Response (IIR) filter which requires only one delay

storage per measurement. With IIR filter, the overall process is similar to a likelihood ratio test with geometric moving average (Basseville & Nikiforov, 1993).

When the above procedure is not sufficient to detect and/or isolate the faults, the state residual and state estimate signals from the Kalman filter are checked. This is needed to detect and isolate the injector fault. The injector fault too could be captured by defining a multiplicative parameter in the model; however, an ad-hoc method using state residuals from the Kalman filter was employed here. Since the injector fault also affects exhaust manifold states and intake manifold states (through EGR), isolation is difficult. The fault detection function g_k for EM leak gives a fairly high value for injector fault too. However, the state correction term Kv_k from Kalman filter can be used to isolate injector fault in one of the cylinders, assuming single fault. The state error correction signal for fuel mass in cylinder with faulty injector will be higher in absolute value than non-faulty ones. The filtered state error correction signal Δm_i for each cylinder fuel mass could be compared with their mean, and if the deviation from the mean is more than a threshold for a particular cylinder, the corresponding injector is faulty.

2.5. Joint State and Parameter Estimation for Fault Identification

Once the fault is detected and isolated, the nominal estimator could be modified to identify only the parameter associated with the detected fault. The estimator error is minimized in the least square sense by updating the parameter at each time step as (Haykin, 2001):

$$w_{k+1} = w_k + r_k \tag{20}$$

Where, w_k is the parameter vector and r_k is a small noise term added for numerical stability of the estimator. The new state vector is formed by appending w_k to the original state vector x_k. The state and measurement equations will now be functions of this combined state and parameter vector. In this paper, only the intake manifold leak area estimation has been performed.

3. SIMULATION RESULTS AND DISCUSSION

The estimation and fault diagnosis techniques described were tested against data generated from an AMESim™ model of the engine with 4 cylinders.

3.1. Estimation of Nominal Engine States

The estimates of nominal engine states using EKF, UKF and RBPF are shown in Figure 3. The UKF uses 50 weights and RBPF uses 12 particles. The normalized root mean square error (NRMSE) was used as a performance indicator and is shown in Table 1. The computation times taken for a 4 second simulation of the engine model and estimator are also given in the table. It is seen that the RBPF and UKF are marginally better in performance than EKF; however, this comes at a much greater computational effort. The UKF, even with more number of weights than number of particles for RBPF, performs worse than RBPF in terms of computation time and estimation accuracy. The EKF could be employed for online estimation on account of its fast execution.

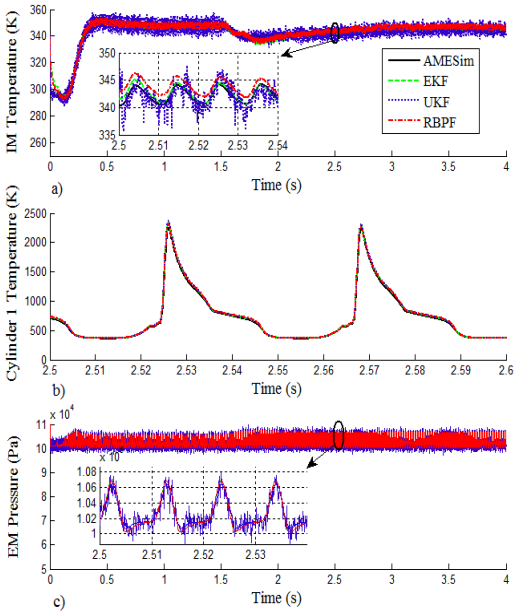

Figure 3. Comparison of state estimates using EKF, UKF and RBPF: a) Intake manifold temperature, b) Cylinder 1 temperature and c) Exhaust manifold pressure

Table 1. Comparison of nominal state estimators

Estimator	NRMSE	Computation Time (s)
EKF	0.0417	55
UKF	0.0412	1360
RBPF	0.0404	620

3.2. Online Fault Detection and Isolation

The EKF estimation based on nominal model was carried out for three kinds of faults considered.

3.2.1. Detection and Isolation of Intake Manifold Leak Fault

An intake manifold leak fault of 50mm^2 area was introduced at 3sec. in the AMESim™ model. The nominal estimator was run with data from AMESim™ simulation. The throttle

signal, residuals from the estimator and fault detection function g_k in Eq.(19), for both IM leak and EM leak are all shown in Figure 4. The threshold value used for g_k was 0.4. It could be seen that the g_k for EM leak is always less than this value and hence, for the fault magnitude of 50mm^2, IM leak is detectable and isolable for low throttle values.

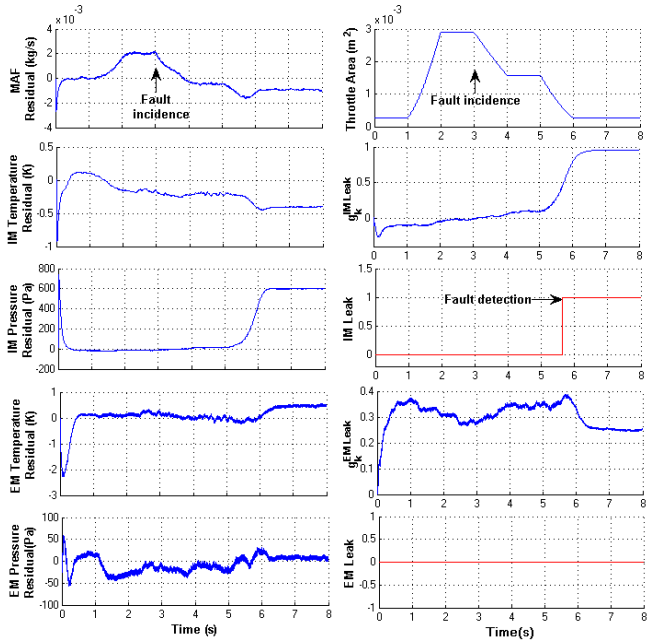

Figure 4. Measurement residuals and fault detection functions in presence of intake manifold leak

3.2.2. Detection and Isolation of Injector Fault

In this case, the data was collected by halving the pulse width of cylinder 1 fuel injector signal. None of the measurements available provides direct data from the cylinders, but EKF is able to estimate the cylinder states. The EM temperature shows a dip at every fourth cycle, which indicates fault with one of the cylinders. The state error correction signals for cylinder masses obtained from the estimator were used to detect the injector fault. The filtered state error correction signals and results of fault detection are shown in Figure 5. It is seen that the fault detection function g_k for EM leak gives a false alarm in this case. To resolve this fault from EM leak, checking the state error correction signal is necessary.

3.2.3. Detection and Isolation of Exhaust Manifold Leak Fault

An exhaust manifold leak fault of 50mm^2 area was introduced at 3sec. in the AMESim^{TM} model. The throttle signal, residuals from the estimator and fault detection function g_k in Eq.(19), for both IM leak and EM leak are all shown in Figure 6. The threshold value used for g_k was 0.4. As pointed out earlier, the g_k for EM leak gives a false alarm for injector fault, and should be resolved by checking mass correction signals from estimator. It could be seen that the g_k for IM leak is always less than that for EM leak and hence, for the fault magnitude of 50mm^2, EM leak is detectable and isolable for low throttle values.

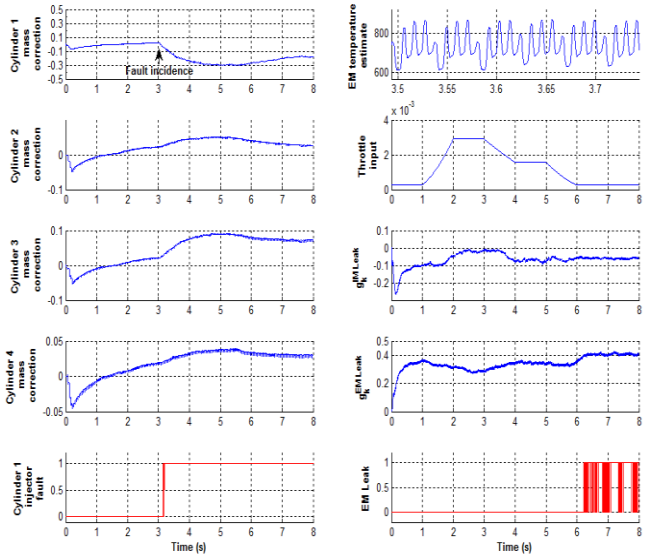

Figure 5. State error correction signals, exhaust manifold temperature and fault detection functions for injector fault

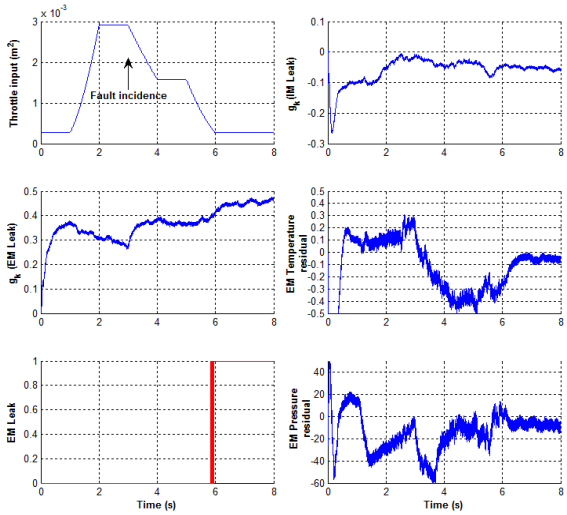

Figure 6. Measurement residuals and fault detection functions in presence of intake manifold leak

3.3. Fault Identification by Joint State and Parameter Estimation

The joint state and parameter estimation was carried out for IM leak fault. To this end, once the leak is detected, a fault flag is sent to the EKF estimator and it is tuned to detect the leak area, now defined as a new state. Once the leak area estimation is started, the fault detection signal for IM leak is no longer valid, since the residuals will now tend to zero.

The fault detection function g_k for IM leak and leak area estimates are shown in Figure 7. For a 50 mm^2 leak fault, the final value of estimated leak is 48.3mm^2 the error in estimation being only 1.7 mm^2.

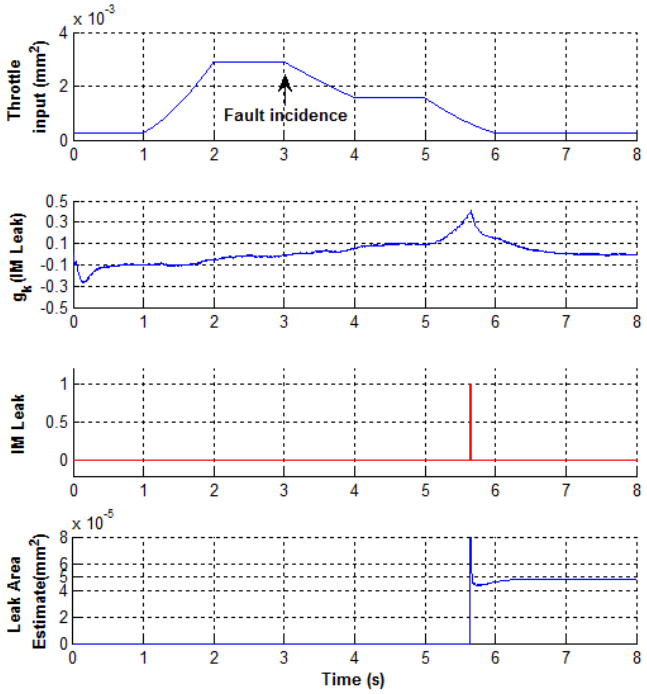

Figure 7. IM leak detection function and leak area estimate

4. CONCLUSION

An Extended Kalman Filter (EKF) based estimator that uses an instantaneous physics based model of the spark ignition automotive engine was shown to be sufficient for online estimation of engine states with estimation accuracy comparable to other nonlinear estimators like Unscented Kalman Filter (UKF) and Rao-Blackwell Particle Filter (RBPF). The use of such an estimator for fault detection and isolation of intake manifold leak, injector fault and exhaust manifold leak was demonstrated. Online identification of faults by tuning the estimator for joint and state and parameter estimation, once a fault is detected, was also demonstrated for the intake manifold leak fault.

ACKNOWLEDGEMENT

Research reported in this publication was supported by National Program for Micro and Smart Systems (NPMASS), Govt. of India.

NOMENCLATURE

A	Area of cross section for flow
C_d	Coefficient of discharge
C_p	Constant pressure specific heat of gases (J/kg K)
C_v	Constant volume specific heat of gases (J/kg K)
C_{pa}	C_p for air (J/kg K)
C_{pb}	C_p of burnt gases (J/kg K)
C_{pf}	C_p of fuel (J/kg K)
C_{va}	C_v for air (J/kg K)
C_{vb}	C_v of burnt gases (J/kg K)
C_{vf}	C_v of fuel (J/kg K)
m	Mass of gas in a reservoir element (kg)
$\dot{m}$	Mass flow rate (kg/s)
P	Pressure (N/m^2)
Q_{LHV}	Lower Heating Value of fuel, accommodating latent heat of vaporization for fuel (J/kg)
$\dot{Q}^{(i)}_{heatloss}$	Convective and radiative heat loss in i^{th} cylinder (J/s)
R_i	Specific gas constant for a material i (J/kgK)
T	Temperature at the reservoir (K)
T_a	Ambient Temperature (K)
T_{cool}	Environment temperature for convection (K)
h_c	Heat transfer coefficient (W/m^2 K)
V	Volume of the element (m^3)
θ	Crank angle (rad)
θ_{soc}	Crank angle for start of combustion (rad)
α	Throttle Angle (rad)
ω	Angular engine speed (rad/s)
γ	Ratio of specific heats for gas
η_c	Combustion efficiency
ρ	Density of gas
λ	Lambda value from lambda sensor
λ_{af}	Stoichiometric air fuel ratio

REFERENCES

Annand, W. J. (1963). Heat transfer in the cylinder of reciprocating internal combustion engines. *Proceedings of the IMechE, Part D: Journal of Automobile Engineering*, (pp. 973–990).

Arulampalam, M. S., Maskell, S., Gordon, N., & Clapp, T. (2002). A tutorial on particle filters for online nonlinear/non-Gaussian Bayesian tracking. *Signal Processing, IEEE Transactions on, 50*(2), 174-188.

Bar-Shalom, Y., Li, X. R., & Kirubarajan, T. (2004). *Estimation with applications to tracking and navigation: theory algorithms and software.* John Wiley & Sons.

Basseville, M., & Nikiforov, I. V. (1993). *Detection of abrupt changes: theory and application* (Vol. 104). Prentice Hall Englewood Cliffs.

De Freitas, N. (2002). Rao-Blackwellised particle filtering for fault diagnosis. *Aerospace Conference Proceedings, 2002. IEEE, 4*, pp. 4-1767.

Doucet, A., De Freitas, N., Gordon, N., & others. (2001). *Sequential Monte Carlo methods in practice* (Vol. 1). Springer New York.

Guzzella, L., & Onder, C. H. (2010). *Introduction to modeling and control of internal combustion engine systems*. Springer.

Haykin, S. S. (Ed.). (2001). *Kalman filtering and neural networks*. Wiley Online Library.

Heywood, J. B. (1998). *Internal Combustion Engine Fundamentals*. McGraw-Hill International Editions.

Hutter, F., Dearden, R., & others. (2003). The gaussian particle filter for diagnosis of non-linear systems. *Proceedings of the 5th IFAC Symposium on Fault Detection, Supervision and Safety of Technical Processes*.

Sarkka, S. (2006). *Recursive Bayesian inference on stochastic differential equations*. Helsinki University of Technology.

Sengupta, S., Mukhopadhyay, S., & Deb, A. K. (2011). Instantaneous within cycle model based fault estimators for SI engines. *India Conference (INDICON), 2011 Annual IEEE*, (pp. 1-6).

Sengupta, S., Mukhopadhyay, S., Deb, A., Pattada, K., & De, S. (2012). Hybrid Automata Modeling of SI Gasoline Engines towards State Estimation for Fault Diagnosis. *SAE International Journal of Engines*, *5*(3), 759-781.

BIOGRAPHIES

Nadeer E P received the B.Tech. degree in Applied Electronics and Instrumentation Engineering from Kerala University, Trivandrum, India in 2006 and M.Tech. degree in Electrical Engineering from the Indian Institute of Technology, Kharagpur, in 2008. During 2008-2010, he worked at SanDisk Semiconductors, Shanghai, China. Since 2010, he has been pursuing his Ph.D degree in the Advanced Technology Development Centre (ATDC), Indian Institute of Technology, Kharagpur.

Amit Patra received the B.Tech., M.Tech. and Ph.D. degrees from the Indian Institute of Technology, Kharagpur in 1984, 1986 and 1990 respectively. During 1992-93 and in 2000 he visited the Ruhr University, Bochum, Germany as a Post-Doctoral Fellow of the Alexander von Humboldt Foundation. He joined the Department of Electrical Engineering, Indian Institute of Technology, Kharagpur in 1987 as a faculty member, and is currently a Professor. He was the Professor In-Charge, Advanced VLSI Design Lab, at IIT Kharagpur during 2004-07. Between 2007 and 2013 he served as the Dean (Alumni Affairs and International Relations) at IIT Kharagpur. His current research interests include power management circuits, mixed-signal VLSI design and embedded control systems. He has guided 17 doctoral students and published more than 200 research papers in various Journals and Conferences. He is the co-author of two research monographs entitled General Hybrid Orthogonal Functions and Their Applications in Systems and Control, published by the Springer Verlag in 1996, and Nano-Scale CMOS Analog Circuits Models and CAD Tools for High-Level Design, published by CRC Press in 2014. Dr. Patra received the Young Engineer Award of the Indian National Academy of Engineering in 1996 and the Young Teachers Career Award from the All India Council for Technical Education in 1995. He has been a Young Associate of the Indian Academy of Sciences during 1992-97. He is a member of IEEE (USA), Institution of Engineers (India) and a life member of the Systems Society of India.

Siddhartha Mukhopadhyay received his B.Tech. (Hons.), M.Tech. and Ph.D., all from IIT Kharagpur in 1985, 1987, and 1991, respectively. He is a professor in the Department of Electrical Engineering, IIT, Kharagpur, at present. His current research interests are in aerospace tracking, guidance and control, estimation and control theory, process monitoring, automotive failure diagnosis and prognosis, industrial automation and behavioral modeling of AMS VLSI circuits for CAD and test development. He is involved with several consulting and research projects in the above areas sponsored by the government research funding agencies of India and the USA, such as DRDO, ISRO, DIT, Ministry of Power, and industrial organizations including SAIL, CESC, General Motors USA, National Semiconductor Corporation, USA, Freescale Semiconductor, USA. He was the Thrust Area Co-lead for IVHM of the General Motors Collaborative Research Lab on Electronic Controls and Software at IIT Kharagpur. Dr. Mukhopadhyay has received the Young Scientist Award from INSA and the Young Engineer Award from INAE. He is a member of the Editorial Board of the Journal of Systems Science and Engineering and the Journal of IETE. He was the National Coordinator of NPTEL-I in the discipline of electrical engineering.